Pulsed, single-frequency, ring laser with a holographic output coupler

Alex Dergachev*

Q-Peak, Inc., 135 South Road, Bedford, Massachusetts 01730 USA
**dergachev@qpeak.com*

Abstract: A unidirectional, passively Q-switched, 2.05-μm Ho:YLF ring laser providing single-frequency, sub-mJ-energy, 100-200-ns-long laser pulses at a kHz rate is reported. The wavelength selection and "coarse" spectral narrowing is performed by utilizing a volume Bragg grating as a resonant, narrowband output coupler operated at a small angle away from normal incidence. Pulsed operation of the Ho:YLF oscillator and further spectral narrowing down to a single longitudinal mode is achieved via passive Q-switching using a Cr^{2+}-doped saturable absorber.

OCIS codes: (140.3560) Lasers, ring; (140.3580) Lasers, solid-state.

References and links

1. H. Kogelnik, "Coupled wave theory for thick hologram gratings," Bell Syst. Tech. J. **48**, 2909–2945 (1969).
2. I. V. Ciapurin, L. B. Glebov, and V. I. Smirnov, "Modeling of Gaussian beam diffraction on volume Bragg gratings in PTR glass," Proc. SPIE **5742**, 183–194 (2005).
3. L. D. DeLoach, R. H. Page, G. D. Wilke, S. A. Payne, and W. F. Krupke, "Transition metal-doped zinc chalcogenides: spectroscopy and laser demonstration of a new class of gain media," IEEE J. Quant. Electron. **32**(6), 885–895 (1996).
4. R. H. Page, K. I. Schaffers, L. D. DeLoach, G. D. Wilke, F. D. Patel, J. B. Tassano, Jr., S. A. Payne, W. F. Krupke, K. T. Chen, and A. Burger, "Cr^{2+}-doped zinc chalcogenides as efficient, widely tunable mid-infrared lasers," IEEE J. Quant. Electron. **33**(4), 609–619 (1997).
5. A. V. Podlipensky, V. G. Shcherbitsky, N. V. Kuleshov, V. P. Mikhailov, V. I. Levchenko, and V. N. Yakimovich, "Cr^{2+}:ZnSe and Co^{2+}:ZnSe saturable-absorber Q switches for 1.54- μm Er:glass lasers," Opt. Lett. **24**(14), 960–962 (1999).
6. T. Y. Tsai, and M. Birnbaum, "Q-switched 2- μm lasers by use of a Cr^{2+}:ZnSe saturable absorber," Appl. Opt. **40**(36), 6633–6637 (2001).
7. A. Di Lieto, P. Minguzzi, A. Toncelli, M. Tonelli, and H. P. Jenssen, "A diode-laser-pumped tunable Ho:YLF laser in the 2 μm region," Appl. Phys. B **58**(1), 69–71 (1994).
8. O. M. Efimov, L. B. Glebov, L. N. Glebova, K. C. Richardson, and V. I. Smirnov, "High-efficiency Bragg gratings in photothermorefractive glass," Appl. Opt. **38**(4), 619–627 (1999).
9. A. Dergachev, P. F. Moulton, V. Smirnov, and L. Glebov, "High power CW Tm:YLF laser with a holographic output coupler," in *Conference on Lasers and Electro-Optics/International Quantum Electronics Conference and Photonic Applications Systems Technologies*, Technical Digest (CD) (Optical Society of America, 2004), paper CThZ3. *http://www.opticsinfobase.org/abstract.cfm?URI=CLEO-2004-CThZ3*
10. B. Jacobsson, M. Tiihonen, V. Pasiskevicius, and F. Laurell, "Narrowband bulk Bragg grating optical parametric oscillator," Opt. Lett. **30**(17), 2281–2283 (2005).
11. B. Jacobsson, V. Pasiskevicius, and F. Laurell, "Single-longitudinal-mode Nd-laser with a Bragg-grating Fabry-Perot cavity," Opt. Express **14**(20), 9284–9292 (2006), http://www.opticsinfobase.org/oe/abstract.cfm?URI=oe-14-20-9284.
12. I. S. Moskalev, V. V. Fedorov, V. P. Gapontsev, D. V. Gapontsev, N. S. Platonov, and S. B. Mirov, "Highly efficient, narrow-linewidth, and single-frequency actively and passively Q-switched fiber-bulk hybrid Er:YAG lasers operating at 1645 nm," Opt. Express **16**(24), 19427–19433 (2008), http://www.opticsinfobase.org/oe/abstract.cfm?URI=oe-16-24-19427.
13. W. R. Sooy, "The natural selection of modes in a passive q-switched laser," Appl. Phys. Lett. **7**(2), 36–37 (1965).
14. Y. Isyanova, and D. Welford, "Temporal criterion for single-frequency operation of passively Q-switched lasers," Opt. Lett. **24**(15), 1035–1037 (1999).
15. D. C. Jones, and D. A. Rockwell, "Single-frequency, 500-ns laser pulses generated by a passively Q-switched Nd laser," Appl. Opt. **32**(9), 1547–1550 (1993).
16. J. E. Hellström, B. Jacobsson, V. Pasiskevicius, and F. Laurell, "Finite beams in reflective volume Bragg gratings: theory and experiments," IEEE J. Quantum Electron. **44**(1), 81–89 (2008).

#142385 - $15.00 USD Received 8 Feb 2011; revised 16 Mar 2011; accepted 17 Mar 2011; published 24 Mar 2011

17. B. Jacobsson, J. E. Hellström, V. Pasiskevicius, and F. Laurell, "Widely tunable Yb:KYW laser with a volume Bragg grating," Opt. Express **15**(3), 1003–1010 (2007), http://www.opticsinfobase.org/oe/abstract.cfm?URI=oe-15-3-1003.
18. B. Jacobsson, C. Canalias, V. Pasiskevicius, and F. Laurell, "Narrowband and tunable ring optical parametric oscillator with a volume Bragg grating," Opt. Lett. **32**(22), 3278–3280 (2007).
19. A. Dergachev, "Ring resonator with holographic reflector," Patent pending.
20. A. E. Siegman, *Lasers* (University Science Books, 1986).
21. D. J. Bradley, C. J. Mitchell, and M. S. Petty, "Direct measurement of the spectral width of a transform-limited ruby laser giant pulse," Opt. Commun. **1**(5), 245–247 (1969).

1. Introduction

Coherent LIDAR applications require pulsed, narrow-linewidth laser sources operating in eye-safe wavelength regions near 1.5 and 2.0 μm. The application requirements for spectral linewidth dictate that the minimum (time-bandwidth limited) laser pulsewidth has to be in 100-300-ns range. Typically such lasers are based on high-energy, injection-seeded, long-resonator, Q-switched oscillators. A promising alternative is an oscillator-amplifier architecture where a low-power, Q-switched, single-frequency laser oscillator is amplified directly to the required energy/power level.

This paper reports on a pulsed, single-frequency, ring Ho-oscillator that generates 100-200-ns pulses at kHz repetition rates with >1 W of average power in the 2-μm wavelength region. Wavelength selection and "coarse" spectral narrowing are accomplished by utilizing a thick holographic grating (i.e. volume Bragg grating) [1,2] as a resonant, narrowband output coupler. Pulsed operation of the Ho-oscillator and further spectral narrowing down to a single longitudinal mode (SLM) is achieved via passive Q-switching using Cr^{2+}-doped saturable absorbers.

Our oscillator design employs a unidirectional ring resonator, which eliminates spatial hole-burning in the laser medium, thereby reducing longitudinal-mode competition and improving energy extraction. It is worth noting that in a passively Q-switched ring cavity emitted photons are passing through the gain medium and the saturable absorber only once per roundtrip (as opposed to two passes in a standing wave cavity) resulting in generation of twice longer pulses than in a standing-wave cavity with the same roundtrip time and the same laser arrangement (laser crystal, saturable absorber, pump power and beam geometry) – a significant benefit in achieving the laser pulsewidth goal set for this development effort.

The absorption properties of Cr^{2+}-doped II-VI materials (first developed as laser media at Livermore National Lab [3,4]) make them suitable for passive Q-switching of Er, Tm, and Ho-doped lasers operating in the 1.5-1.6-μm and 1.9-2.1-μm wavelength regions. The use of Cr^{2+}-doped media as saturable absorbers was reported shortly after for passive Q-switching of 1.5-μm Er:glass laser [5] and 2-μm Ho:YAG and Tm:YAG lasers [6].

Our choice of 2-μm Ho-doped laser material (as opposed to 1.5-μm Er-doped lasers) is based on the fact that the much higher gain of Ho-doped crystals allows efficient further amplification of a pulsed seed oscillator to provide the desired scaling of eye-safe laser output. This approach decreases the number of amplifying stages, simplifies the overall design and improves the electrical efficiency of the complete laser system as compared to Er-doped laser technology.

2. Ring laser resonator with a holographic output coupler

2-μm-wavelength, Ho-doped materials have a tuning range of up to several 10's of nm [7]. In order to lock the laser to a desired wavelength and to provide "coarse" narrowing of the spectral output of the ring oscillator, we utilized a narrowband, resonant output coupler based on a reflective thick holographic grating instead of a dielectric partial reflector. An example of such holographic element is a volume Bragg grating (VBG) recorded in photo-thermo-refractive glass [8].

VBGs are widely used in laser design as spectrally selective reflectors in standing-wave cavities applicable to either active laser [9] or nonlinear optical devices (OPOs) [10]. Such

#142385 - $15.00 USD Received 8 Feb 2011; revised 16 Mar 2011; accepted 17 Mar 2011; published 24 Mar 2011

thick holographic reflectors are typically operated at normal incidence (see Fig. 1a) either as high reflectors or output couplers.

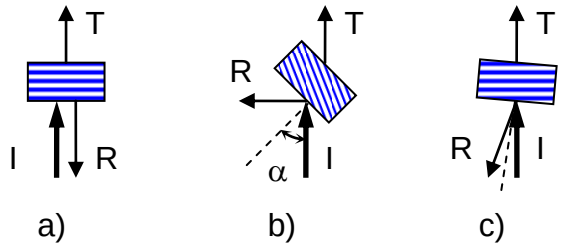

Fig. 1. Operation of thick holographic gratings in laser resonators: a) Normal incidence – provides maximum angular acceptance and is utilized in standing-wave resonators, b) Large angle of incidence in the range of 5 to 85 deg – more than 10x reduction in angular acceptance *vs.* normal incidence, c) Small angle of incidence 0.5-2 deg – only 2-5 times reduction in angular acceptance *vs.* normal incidence (this work).

A narrowband VBG reflector can be used for selection of a single longitudinal mode in a cw laser with a short (<8 mm) standing-wave cavity as demonstrated in Ref [11]. for a Nd:$GdVO_4$ laser. However, in a pulsed (actively Q-switched) standing-wave laser with a relatively long resonator length (>100 mm) just a single VBG reflector cannot assure SLM operation [12]. A simple solution to facilitate the generation of a single longitudinal mode in a pulsed laser is to utilize passive Q-switching [13,14]. When the active Q-switch in Ref [12]. was replaced with a passive Q-switch the laser reliably operated on a single longitudinal mode. It is worth pointing out that a passively Q-switched laser may benefit from the use of a VBG reflector (e.g. for wavelength locking) but does not necessarily need it to achieve SLM regime. Typical passively Q-switched lasers (excluding microchip oscillators) with a standing-wave resonator produce laser pulses with 1-100-ns width and to lengthen the pulse (reduce the spectral linewidth) one should increase the resonator length to 100's of cm making the laser bulky and less reliable [15]. An alternative is to consider a ring resonator architecture the benefits of which are described in Section 1 above.

In principle, thick holographic reflective gratings can be designed to operate at an angle (see Fig. 1b) but the key issue in this case is the significant narrowing of the VBG angular acceptance with the increase of the angle of incidence leading to reduction in the VBG reflectivity and beam profile distortion [16]. A small angular acceptance requires the use of large, collimated beams with very low divergence. Nevertheless the operation of a standing-wave, narrowband, continuously tunable Yb:KYW laser locked by a VBG at oblique incidence (internal angle of incidence ~10-20 deg) in a retro-reflector configuration was reported [17]. As far as a ring resonator layout is concerned, we are aware of only one publication that demonstrated a ring OPO utilizing a retroreflector element based on a VBG output coupler [18]. However, the VBG was operated at a large angle of incidence of ~20 deg (internal) and the minimum beam diameter for the resonator mode (limited by the VBG angular acceptance) was estimated to be ~520 μm [18].

In order to incorporate a holographic output coupler in a ring resonator without sacrificing the angular acceptance we chose to operate the VBG at a small angle of incidence (see Fig. 1c) and developed a novel ring resonator scheme as shown in Fig. 2 [19]. Details of the VBG design and particular characteristics are discussed below for a Ho:YLF ring oscillator operating at 2.05 μm, however, this approach can be applied for any laser medium.

The key objective to incorporate a holographic reflector in a ring resonator is achieved by utilizing a VBG element which is designed to support the desired operational wavelength not at normal incidence but at a small Bragg angle in the 0.5-2 degree range. Deviation of the Bragg angle (BA) from normal incidence strongly affects the angular acceptance of a VBG element but has almost no effect on its spectral bandwidth [1,2].

#142385 - $15.00 USD Received 8 Feb 2011; revised 16 Mar 2011; accepted 17 Mar 2011; published 24 Mar 2011

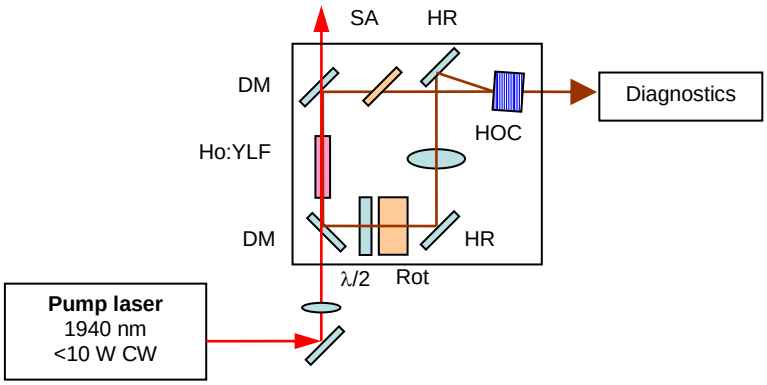

Fig. 2. Schematic layout of the ring Ho:YLF oscillator (HOC –holographic output coupler, SA - saturable absorber, DM – dichroic mirror, HR – high reflector, Rot - Faraday rotator).

As indicated in Ref [2]. a reflective VBG has its largest angular acceptance bandwidth as long as the incident Bragg angle is not exceeding a "threshold" value defined as: $\tan^2\theta_0 = 2\delta\lambda^{HWFZ}/3\lambda_0$ (see Ref [2].), where $\delta\lambda^{HWFZ}$ is the wavelength difference between the central peak and the first zero in the dependence of diffraction efficiency *vs.* wavelength detuning from the design wavelength λ_0 (see Fig. 3).

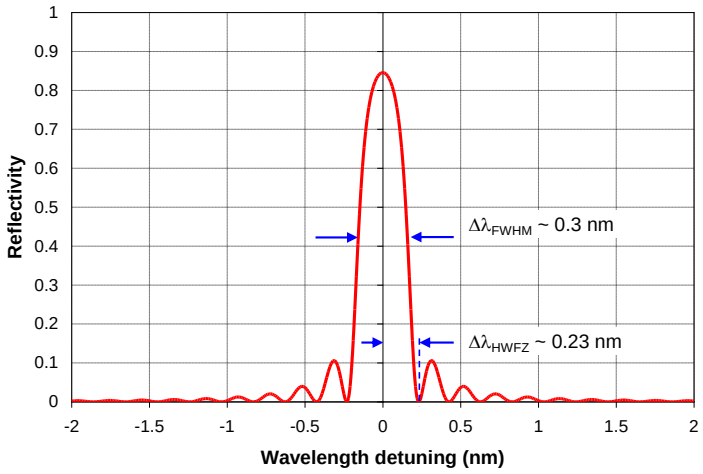

Fig. 3. Calculated reflectivity at normal incidence vs wavelength detuning for a VBG element with resonance wavelength of 2051 nm, ~7-mm thickness and 150-ppm index modulation. The full-width at half-maximum (FWHM) for the reflectivity peak is ~0.3 nm. The half-width at first zero (FWHZ) is ~0.23 nm.

Based on the data from Fig. 3 ($\delta\lambda^{HWFZ}$ ~0.23 nm at λ~2.05 μm) we can calculate the "threshold" angle as ~0.5 deg. If the design Bragg angle is increased beyond the threshold value the angular acceptance bandwidth rapidly decreases. This is illustrated in Fig. 4, which shows the dependence of VBG diffraction efficiency on the angle of incidence for four different values of the design Bragg angle (0 deg (normal incidence), 1, 2 and 4 deg). Assuming a VBG with a maximum reflectivity of ~85% at 2.05 μm, the calculated angular bandwidth for Bragg reflection peak (FWHM) is ~9 mrad for BA = 1 deg, ~4.3 mrad at BA = 2 deg, and ~2.2 mrad at BA = 4 deg (see Fig. 4). These diffraction efficiency calculations are based on the analysis of reflective thick holographic gratings using the plane-wave approximation provided in Ref [1].

#142385 - $15.00 USD Received 8 Feb 2011; revised 16 Mar 2011; accepted 17 Mar 2011; published 24 Mar 2011

A larger angular bandwidth for the Bragg reflector is advantageous as it allows to design less misalignment-sensitive ring resonators, improves wavelength stability and simplifies the laser assembly. On the other hand the VBG output coupler should be designed to operate at an angle of incidence large enough to provide sufficient angular separation between the incident and reflected beams so that ring resonator can be constructed. The ultimate upper limit on the design Bragg angle for a VBG element is determined by the divergence of the lasing mode in a particular resonator: the beam divergence should not exceed the angular acceptance bandwidth of a VBG reflector.

The VBG reflector for this effort was designed to provide ~80-90% reflectivity near 2.05 μm at a 1-1.5 deg Bragg (internal) angle with spectral selectivity of 0.25-0.3 nm (FWHM) and was fabricated by Optigrate, Inc. The VBG resonance wavelength near 2.05 μm corresponds to the strongest emission peak in Ho:YLF. Also the narrow spectral bandwidth of VBG element prevents lasing at 2.06 μm (which occurs first in Ho:YLF lasers at low inversion levels and low output coupling) regardless of the pump power.

3. Laser experiments and results

The Ho:YLF ring oscillator set-up (see Fig. 2) was based on longitudinal pumping scheme. All resonator mirrors were flat, 45-deg high reflectors at 2.05 μm. A single spherical lens (+200 mm focal length, fused silica) AR-coated at 2.05 μm was used to assure stability of the ring cavity. Based on ABCD-matrix formalism the diameter of fundamental mode in the laser crystal for ~30-cm-long ring resonator was calculated to be ~700 μm and the far field divergence (full angle) for the output beam transmitted through the VBG output coupler was ~3.75 mrad. The holographic output coupler (VBG) was operated at an angle of incidence (external) $\alpha = 2$ deg which corresponds to ~1.3-deg internal angle of incidence in the medium. The angular acceptance of VBG reflector at a 1.3 deg internal angle is calculated to be ~7 mrad and is almost twice larger than the divergence of the ring resonator mode. The separation of the VBG reflector and the closest 45-deg HR mirror was ~28 mm.

A single, 30-mm-long, AR-coated, 0.5% Ho:YLF crystal was pumped from one side by a Tm-fiber laser (IPG Photonics) wavelength-adjusted to the strongest Ho:YLF absorption line at 1940 nm. The pump Tm-fiber laser produced a collimated, linearly-polarized, diffraction-limited beam with less than 2-nm linewidth and a maximum average power of ~10 W. Unidirectional operation of the ring resonator was achieved with an intra-cavity optical "diode" based on a Faraday rotator and a waveplate. The Ho:YLF crystal mount was temperature controlled using a thermoelectric element. The ratio of pump to laser wavelengths is ~0.95, indicating that about 5% of the pump power is dissipated as heat. The very modest amount of heat in the Ho:YLF crystal leads to minimal thermal distortion and stresses - all benefits for stable operation in single-frequency regime.

#142385 - $15.00 USD Received 8 Feb 2011; revised 16 Mar 2011; accepted 17 Mar 2011; published 24 Mar 2011

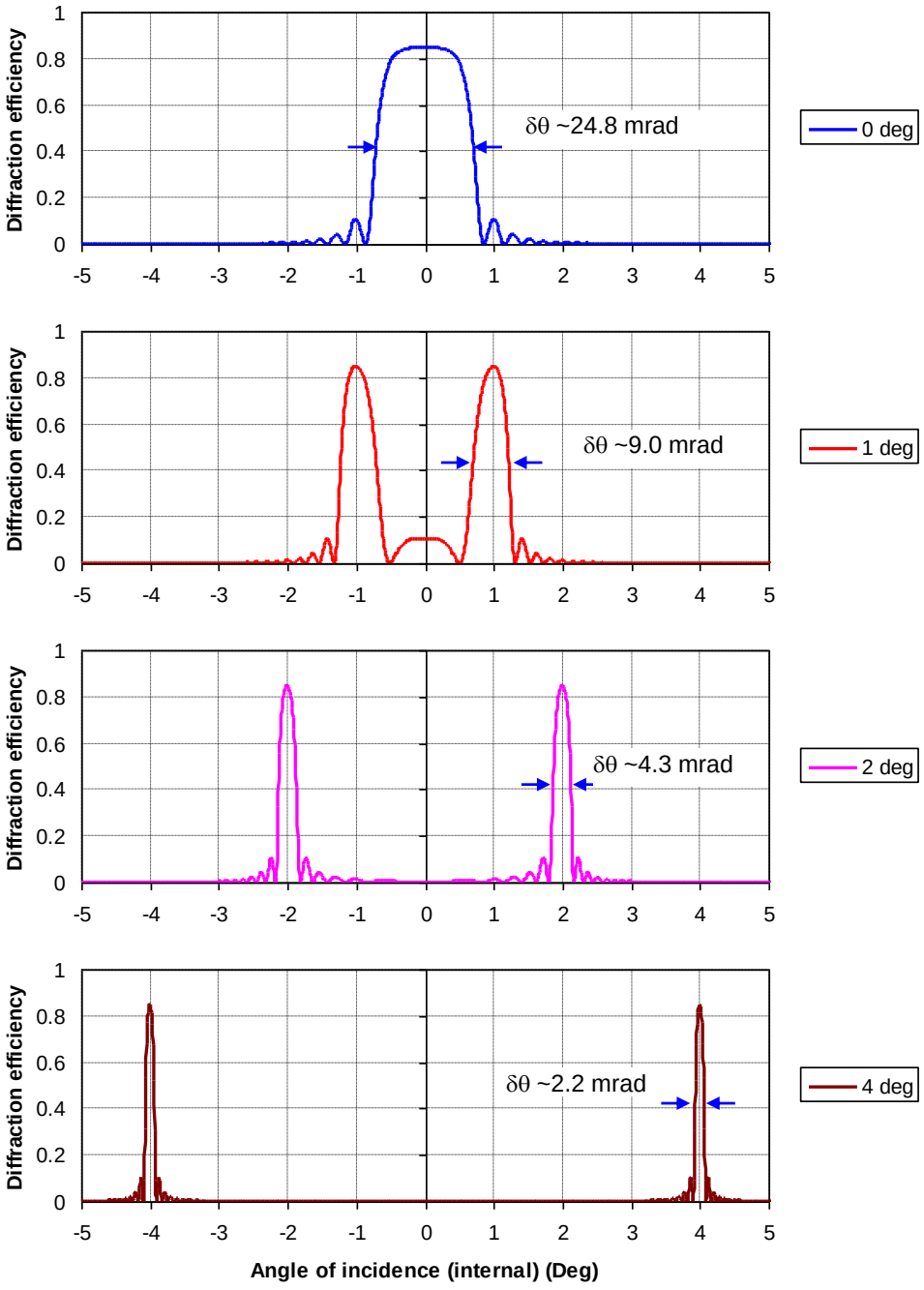

Fig. 4. Calculated diffraction efficiency *vs.* internal angle of incidence for VBG elements at the same resonance wavelength (2051 nm) and the same reflectivity maximum (R~85%) but different Bragg angle (0, or 1, or 2, or 4 deg). 0 deg corresponds to normal incidence. Both ("+" and "-") diffraction orders are shown for angles of incidence other than 0 deg. At normal incidence both orders merge into one peak providing the largest angular acceptance.

#142385 - $15.00 USD Received 8 Feb 2011; revised 16 Mar 2011; accepted 17 Mar 2011; published 24 Mar 2011

Several Cr^{2+}:ZnSe saturable absorbers were ordered from Photonics Innovations, Inc. (now part of IPG Photonics). A passive Q-switch element with initial transmission of T_0~95% at ~2.05 μm was utilized in the experiments described here. The 1.6-mm-thick crystal was operated at Brewster's angle (67.8 deg at 2.05 μm). The initial transmission was characterized at the Brewster angle of incidence. (Alternatively one can use an AR-coated crystal design.)

The Ho:YLF ring oscillator operated in TEM_{00} mode and produced average power output of up to 1.9 W in CW and 1.4 W Q-switched regimes at maximum pump power of ~9 W. The ratio of average power in Q-switched regime to that in CW regime is ~0.74. For VBG reflectivity of ~85% and initial transmission of saturable absorber of ~95% the maximum repetition rate reached ~3.3 kHz and the maximum attainable pulse energy of 0.42 mJ while maintaining single-frequency laser operation. The pulse-to-pulse amplitude stability was measured to be +/– 2.3% and the pulse period stability (pulse jitter) – +/– 2 μs at 3.3 kHz rate.

Figure 5 shows the beam profile for a free-propagating beam from the Ho:YLF ring laser operated at maximum pump power and measured 1.1 m away from the laser resonator waist. The beam profile can be closely approximated by a Gaussian fit (0.955 average correlation) and the measured full beam divergence (~3.9 mrad average) is very close to the estimate obtained from ABCD-matrix calculations (3.75 mrad). We note that thermal lensing in Ho:YLF crystal is very weak and was neglected in the ABCD-matrix calculations.

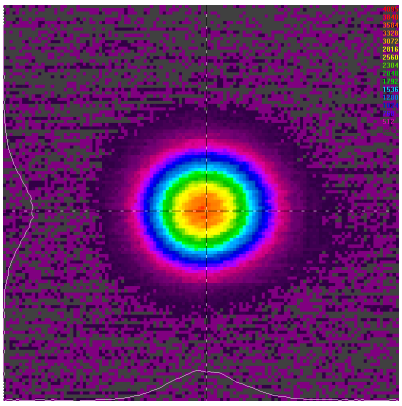

Fig. 5. Measured profile for the free-propagating beam from the Ho:YLF ring laser at maximum pump power. The beam full width and fit to Gaussian are 4.5 mm and 0.95 for horizontal direction and 4.0 mm and 0.96 for vertical direction, respectively.

The dependence of output pulse energy and pulse repetition rate for the ring Ho:YLF oscillator appears in Fig. 6. The laser pulse energy exhibited a non-linear dependence on the pump power, increasing by ~1.6 times from 0.26 to 0.42 mJ as the pump power increased from ~4.5 W to 9 W (see Fig. 6). The dependence of the repetition rate *vs.* pump power can be closely approximated by a linear fit with ~600 Hz/W slope. The laser pulsewidth exhibited a slight dependence on the pump power, showing a decrease from ~175 ns to ~140 ns as the pump power increased from ~4.5 W to 9 W. This pump power change corresponded to the increase of the repetition rate from ~0.6 kHz to ~3.3 kHz (or the decrease of the pulse period from ~1600 μs to ~300 μs). The laser pulsewidth could be easily increased (up to ~200 ns) or decreased (down to ~100 ns) by adjusting the resonator length.

#142385 - $15.00 USD Received 8 Feb 2011; revised 16 Mar 2011; accepted 17 Mar 2011; published 24 Mar 2011

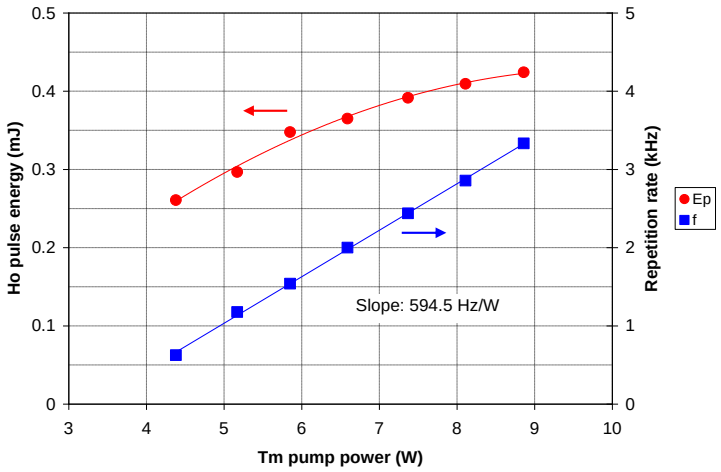

Fig. 6. Pulse energy (circles) and repetition rate (squares) *vs.* pump power for a ring Ho:YLF oscillator with VBG output coupler and ~95%-transmissive Cr^{2+}:ZnSe saturable absorber.

The lasing wavelength of the ring oscillator was measured to be 2050.39 nm. Introduction of an uncoated etalon (as a temporary element) in the laser cavity allowed the tuning of +/– 72 pm away from the central laser wavelength. No attempt was made to carefully study the continuity of fine wavelength tuning with the etalon. This tuning experiment allowed to estimate the spectral bandwidth supported by the particular VBG element in the ring resonator to be ~140 pm, about one half of the calculated spectral bandwidth at FWHM (see Fig. 3).

The spectral narrowing in passively Q-switched oscillators is explained by relatively long time it takes for the laser oscillation to build up from noise to the level sufficient for saturable absorber bleaching [13]. The buildup time in passively Q-switched lasers can be orders of magnitude larger than for active Q-switching and even a small differential loss leads to strong longitudinal mode discrimination due to the increased number of resonator round-trips. The mechanisms of spectral narrowing are discussed in detail in Refs [13,14].

In this work the spectral properties of the Ho:YLF laser oscillator were studied by two common methods to confirm the single-frequency regime of operation. The first method was based on the detection of mode beating in temporal domain utilizing a photodetector and oscilloscope (both with sufficient bandwidth to resolve the sub-ns modulation) [20]. The second method was based on the analysis of the fringe pattern produced by a fixed-length Fabry-Perot interferometer and recorded with a 2D array detector.

For temporal/ fast Fourier transform (FFT) pulse measurements we utilized a fast PIN InGaAs detector (spectral range of 830-~2100 nm, cutoff frequency of ~10 GHz and rise/fall time of <35 ps) and an oscilloscope with ~6-GHz bandwidth. The photodetector/oscilloscope combination allowed us to resolve mode beating at up to ~6 GHz level, which was more than sufficient for characterization of our ring oscillator with a typical mode spacing of ~1 GHz.

The examples of experimental oscilloscope traces are shown in Fig. 7. A portion of a pulse at the peak is shown in Fig. 7a for a single-frequency lasing (no mode beating) in nominal operating regime and in Fig. 7b for a multi-frequency lasing (strong mode beating) from the Ho:YLF oscillator. Multi-frequency pulses were obtained by tapping on one of the resonator mirror mounts to disturb the laser cavity. Both Figs. 7a and 7b also show the FFT curves. The distinct FFT peak at 957 MHz in Fig. 7b corresponds to the mode spacing of our laser resonator (optical length of 32 cm), however, this peak is completely missing for a single frequency pulse (Fig. 7a). Figure 8 shows a high-resolution view (including actual data points) of a 20-ns-wide portion of a multi-frequency pulse trace in Fig. 7b. The modulation period of the pulse trace is ~1.0-ns and the data point interval is 50 ps.

#142385 - $15.00 USD Received 8 Feb 2011; revised 16 Mar 2011; accepted 17 Mar 2011; published 24 Mar 2011

Visualization of the temporal mode beating and subsequent fast Fourier transform provides a simple, fast and reliable way of confirmation if the generated laser pulses are single frequency or not.

Interferometer fringe measurements provided the second method to confirm the single-frequency operation. The plano-plano, air-spaced Fabry-Perot interferometer had fixed 2.2-cm spacing between the mirrors corresponding to the free spectral range of ~6.8 GHz. The resolution of the interferometer set-up was limited to ~200 MHz which and was sufficient to resolve the mode spacing of ~1 GHz.

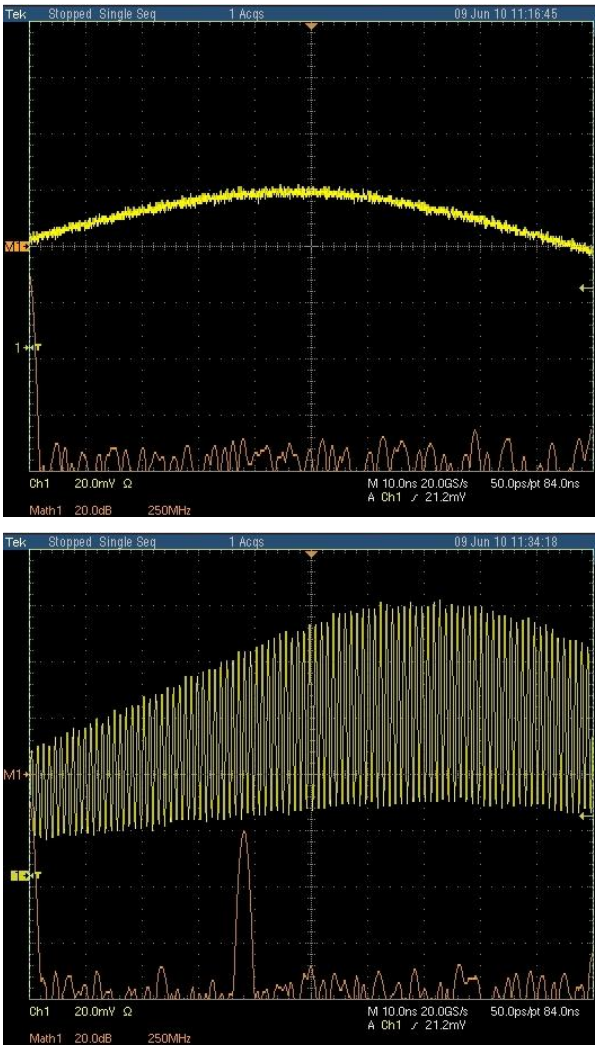

Fig. 7. Zoomed-in oscilloscope traces (yellow) and FFT curves (brown) for (a) a single-frequency pulse, and (b) a multi-frequency pulse from the Ho:YLF oscillator. For FFT curves full-window width corresponds to the frequency span of 2.5 GHz.

#142385 - $15.00 USD Received 8 Feb 2011; revised 16 Mar 2011; accepted 17 Mar 2011; published 24 Mar 2011

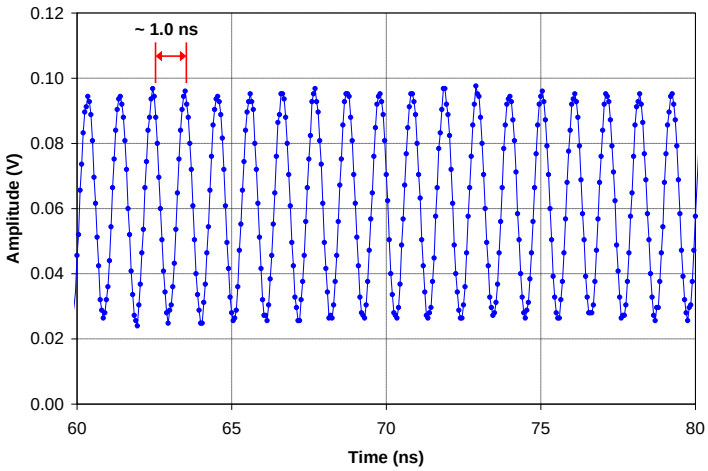

Fig. 8. High-resolution view (20-ns-wide window) of a multi-frequency laser pulse trace in Fig. 7b. The data point interval is 50 ps.

The spectral linewidth of the single-frequency, passively Q-switched Ho:YLF oscillator is estimated to be transform-limited. Such assumption is typical for passively Q-switched lasers and it was experimentally verified in Refs [15,21]. Currently we are in the process of setting up an experimental set up (similar to one described in Ref [15].) to provide direct, high resolution measurement of the spectral linewidth of a pulsed Ho:YLF laser.

4. Conclusion

In conclusion, laser operation of a 2.05-μm, single-frequency, passively Q-switched, bulk Ho:YLF oscillator based on a novel unidirectional ring resonator under 1.9-μm pumping was demonstrated and characterized. Long (140-175 ns), single-frequency laser pulses with pulse energy of ~0.4 mJ at up to 3.3 kHz repetition rate were generated in a Ho:YLF ring oscillator. Such a pulsed, low-average-power laser can be used as a master oscillator in several remote-sensing applications, particularly in coherent LIDAR transmitters. Addition of a high-gain Ho-doped-crystal amplifier stage allows easy scaling to multi-mJ pulse energies. Given the nature of the bulk crystal amplifiers, they provide damage-free operation and are immune to nonlinear effects such as Brillouin and Raman scattering which adversely affect the amplification of single-frequency seed sources in fiber amplifiers.

Acknowledgments

This work was supported by NASA SBIR grant NNX10CE95P. The author is very grateful to Drs. Vadim Smirnov and Igor Ciapurin of Optigrate, Inc. for their efforts in VBG design and fabrication, and to Prof. Sergey Mirov for providing various Cr^{2+}-doped samples.

#142385 - $15.00 USD Received 8 Feb 2011; revised 16 Mar 2011; accepted 17 Mar 2011; published 24 Mar 2011